JOURNAL OF SPACECRAFT AND ROCKETS
Vol. 36, No. 4, July–August 1999

Electrical Breakdown of Anodized Coatings in Low-Density Plasmas

J. T. Galofaro*
NASA Lewis Research Center, Cleveland, Ohio 44135
C. V. Doreswamy†
Tuskegee University, Tuskegee, Alabama 36088
B. V. Vayner‡
Ohio Aerospace Institute, Cleveland, Ohio 44135
and
D. B. Snyder§ and D. C. Ferguson¶
NASA Lewis Research Center, Cleveland, Ohio 44135

A comprehensive set of investigations has been performed involving arcing on a negatively biased anodized aluminum plate immersed in a low-density argon plasma at low pressures ($P_0 \approx 7.5\times10^{-5}$ torr). These arcing experiments were designed to simulate electrical breakdown of anodized coatings in a low-Earth orbital environment. When electrical breakdown of an anodized layer occurs, an arc strikes, and there is a sudden flux of electrons accelerated into the ambient plasma. This event is directly followed by ejection of a quasineutral plasma cloud consisting of ejected material blown out of the anodized layer. Statistical analysis of plasma cloud expansion velocities has yielded a mean propagation velocity, $\nu = 19.4 \pm 3.5$ km/s. As the plasma cloud expands into the ambient plasma, energy in the form of electrical noise is generated. The radiated electromagnetic noise is detected by means of an insulated antenna immersed in the ambient plasma. The purpose of the investigations is 1) to observe and record the electromagnetic radiation spectrum resulting from the arcing process, 2) to make estimates of the travel time of the quasineutral plasma cloud based on fluctuations to several Langmuir probes mounted in the ambient plasma, and 3) to study induced arcing between two anodized aluminum structures in close proximity.

Nomenclature

C = capacitance, F
D = plate separation, m
E = electrical field strength, V/m
f = frequency, Hz
L = antenna length, m
N_e = electron number density, m^{-3}
OD = outer diameter, m
P_0 = neutral gas pressure, torr
R = resistance, Ω
r = probe and plate distance, m
T_e = electron temperature, eV
V = bias potential, V
v = average velocity, m/s
W = width, m
Δx = thickness of anodized layer, m
$\Delta\tau$ = propagation time, s
ν = mean velocity, m/s
ϕ_b = plate bias potential, V

Introduction

THE trend for modern day satellite payloads is for more robust, higher voltage power systems. Where older payloads typically operated at less than 80 V, newer payloads currently operate at just under 200 V. The higher voltages have placed a heavier demand on spacecraft power systems, and the trend is ever increasing as payloads become more complex. Historically spacecraft have incorporated a negative grounding scheme into their structures to provide a single point ground connection for electrical components. The typical way of providing a negative ground is to tie the negative end of the solar array directly to the structure of the spacecraft.The negative grounding scheme has led to other potentially hazardous problems involving arcing. Furthermore, both the solar arrays and the structure are vulnerable to arcing. These arcing concerns have led to other matters involving electromagnetic interference (EMI) with scientific payloads, which also need to be addressed. For example, to provide the required power for the International Space Station (ISS), the operating voltage was set to 160 V (Ref. 1). This 160 V, coupled with the negative grounding scheme, has unfortunately placed the ISS in a region where there are significant physical interactions with the low-Earth-orbit (LEO) plasma.[1–3] The series of experiments will focus on one such interaction, the electrical breakdown of anodized coatings (i.e., structures) in a LEO environment.

Insulating paints often are used to regulate passively the surface temperature of spacecraft structures in LEO.[4,5] More recently several types of anodized coatings have been developed for use on the ISS. A chromic-acid anodized coating, produced by the type I or type IB process, with a thickness between 1.3–5.1 μm was finally decided upon for the ISS.[1,6] The thickness of these coatings has been manufactured to supply the needed thermal properties for temperature stabilization of external surfaces, as well as providing protection against atomic oxygen degradation.

The 160-V solar array of the ISS will cause the structure to charge between −120 and −140 V relative to local plasma potential.[1,2] Unfortunately, the thickness of the anodized surfaces specified for the ISS does not have sufficient dielectric strength to be able to stand off the −120 to −140 V they may acquire.[1,7,8] To fix its problems, the ISS has baselined the use of a plasma contactor. Depending on the design voltage specified for new high-voltage power systems, future spacecraft may need to use thicker anodized coatings to protect against such interactions.

Received 15 September 1998; revision received 14 December 1998; accepted for publication 15 December 1998.

*Physicist, Photovoltaic and Space Environments Branch; joel.t.galofaro@lerc.nasa.gov. Member AIAA.
†Professor.
‡Senior Research Associate, Photovoltaic and Space Environments Branch. Member AIAA.
§Physicist, Photovoltaic and Space Environments Branch. Member AIAA.
¶Senior Scientist, Photovoltaic and Space Environments Branch. Member AIAA.

Experimental Test Apparatus

Ground tests were performed at NASA John H. Glenn Research Center at Lewis Field (LeRC) Plasma Interaction Facility. All of the experiments were conducted in the 1.8-m-diam × 3.0-m-high vertical vacuum chamber. Two Penning discharge sources, equipped with a 0.25-mm-diam tungsten filament, were used to ionize argon gas molecules and provide plasma for the experiments. Neutral gas pressures were carefully monitored and maintained at $P_0 = 7.5 \times 10^{-5}$ torr throughout the tests with the plasma sources operating. Plasma densities N_e ranged between 1.8×10^5–8.6×10^5 electrons/cm^3, and electron temperatures T_e were on the order of 1.2–1.3 eV.

For these experiments several type II, class 1, sulfuric acid anodized aluminum plates, with an alloy designation of 6061-T6 (having a specified minimum coating thickness of 2.5146 μm[1] and conforming to MIL-A-8625E), were procured. The T-6 coating designation calls for tempering an aluminum alloy by heat treatment prior to anodizing a coating electrolytically in a sulfuric acid bath.

The anodized aluminum plates arrived as six precut 30.48 × 30.48 cm plates and one large 60.96 × 60.96 cm plate, which were anodized on both sides. The center conductor of a shielded coaxial cable (RG-58/U, 50Ω) was attached to each plate and terminated with a standard bayonet nut connector (BNC) on the other end. The anodized plates were prepared by covering the sides and back with a 0.05-mm kapton sheet. The plates were then cleaned with an isopropyl alcohol wash and allowed to air dry prior to mounting them in the tank. The BNCs were attached to an insulated electrical feedthrough rated at 1000 V breakdown potential.

Diagnostic equipment consisted of two spherical Langmuir probes (1.9-cm diam) and two cylindrical wire probes (0.32 cm diam × 5.08 cm long). Two antennae were constructed, each with 0.32-cm-diam × 56.56-cm-long insulated whips, and identical 47 × 47 cm hexagonal ground planes that were fashioned from 0.32-cm aluminum sheet metal. A very sensitive current probe amplifier and current probe were also used. Dual-channel (300 and 330 MHz) digitizing oscilloscopes, each equipped with an IEEE-488 bus, also were used to capture and store measurements in a very short time interval.

The mounting positions of the probes inside the vacuum chamber are shown in Fig. 1. All probes, with the exception of antenna B, are mounted at a height of 59.69 cm high off the subfloor of the vacuum tank. Table 1 identifies the measured distance of each probe with respect to the center of the anodized plate.

Figure 2 shows a pictorial diagram of the experimental apparatus used in obtaining the electromagnetic frequency spectrum and for the plasma cloud propagation tests. The diagram shows an anodized aluminum plate biased negative of tank ground by a high-voltage dc power supply. The dc power supply charges a 0.47-μF capacitor, which is mounted in parallel with the dc power supply and the anodized plate. The value of the capacitor is used to represent the capacitance of a typical satellite in space. Note that, when electrical breakdown of the anodized coating occurs, an arc strikes, and the arc return path is through the plasma and back to tank ground. For charge to be conserved, the same current must flow from the negative terminal of the capacitor and back to the anodized plate. A current probe is placed between the negative capacitor terminal and the plate in order to detect an arc. When the current probe detects an arc, the signal is amplified and sent to channel 2, which has been set to trigger at a given current level. Channel 2 of the first scope then simultaneously triggers channel 1 and both channels on the second scope via an external trigger. In this way four channels of information are gathered at once.

The diagram in Fig. 3 depicts the experimental setup used for the induced arcing experiments. For these experiments identical pairs of anodized aluminum plates were mounted in parallel (with the exposed anodized surfaces of the plates facing one another) and floated in the ambient plasma. Note that there are two arcing circuits shown. Each plate is independently biased negative relative to tank ground through a separate dc power supply. An initial arc on plate A simultaneously triggers both channels on the scope.

Table 1 Probe dimensions and mounting positions specified for the verical chamber tests[a]

Probe #	Probe type	Dimension, cm	Distance, cm
LP1	Wire probe 1	$0.3175OD \times 5.08L$	$r = 57.15$
LP2	Spherical probe 2	$1.905OD$	$r = 48.89$
LP3	Wire probe 2	$0.3175OD \times 5.08L$	$r = 77.47$
LP4	Spherical probe 1	$1.905OD$	$r = 78.74$
A & B	Antenna lead	$0.3175OD \times 56.96L$	$r = 100$
	Hexagonal ground plane	47×47	——
Plate 1	Large anodized plate	$60.96L \times 60.96W$	——
	Parallel anodized plates	$18L \times 18W$	$D = 25, 50$

[a]Note: All radii (r) are measured from the center of plate 1, D = plate separation distance, and OD = outer diameter.

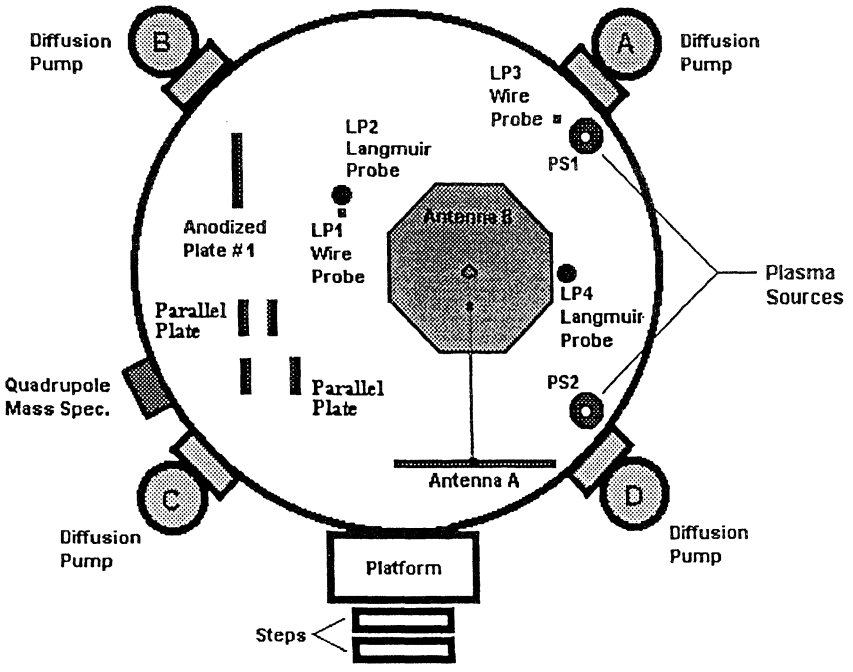

Fig. 1 Top down cutaway view of the vertical chamber (dimensions: 1.8 m in diameter × 3.0 m high).

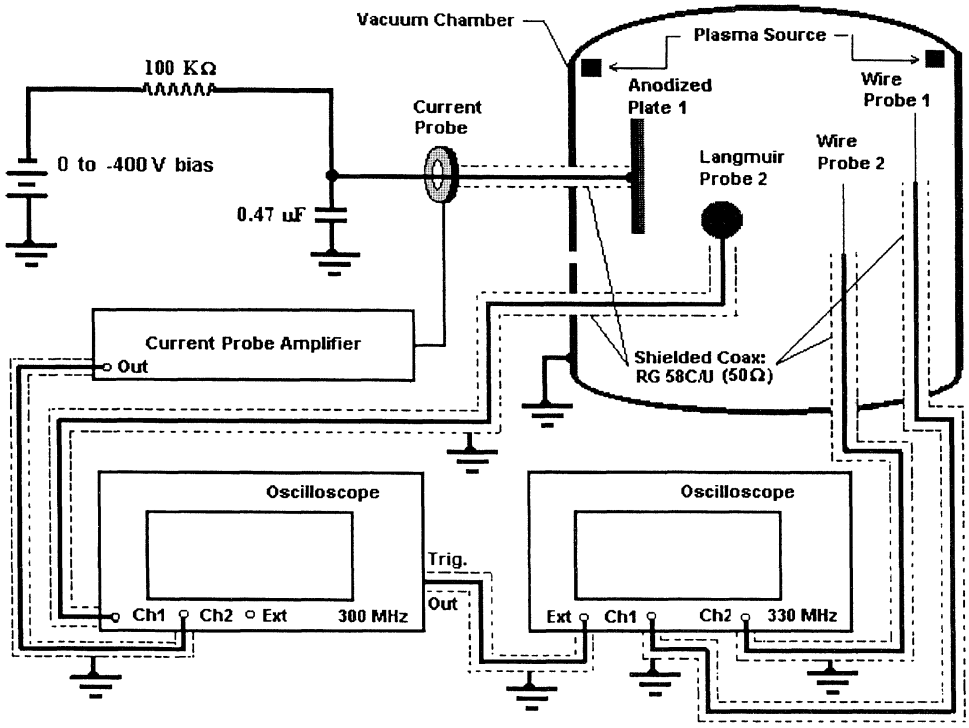

Fig. 2 Experimental apparatus for the electromagnetic frequency spectrum measurements and plasma cloud propagation experiments.

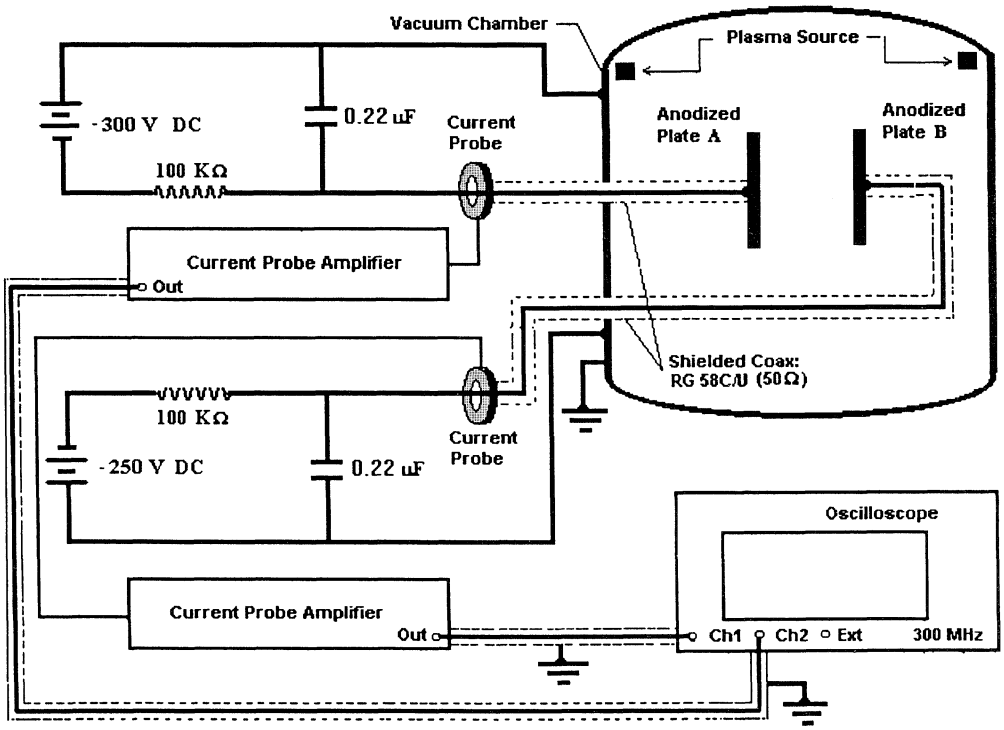

Fig. 3 Experimental apparatus for the induced arcing experiments.

Experimental Results

Measurements of the electromagnetic radiation spectrum resulting from the arcing process were obtained. Being only interested in obtaining EMI measurements generated by the arcing process, the antenna whips needed to be insulated, thereby passing all radiated emissions and effectively blocking the conducted emissions caused by the expansion of the plasma cloud into the ambient plasma.

Both antennae were cut to a resonant frequency of 500 MHz to give a broadband behavior at the measured frequencies. The antenna leads were cut according to the equation $L = 299.8(0.95)/f$, where L is the length in meters and f is the frequency in megahertz. All data were obtained in digital form with a sampling interval of 2.5 ns. This sampling rate yields a maximum bandwidth of 200 MHz for the tests. A fast Fourier transform was applied to the data to map signals from the time domain to a frequency domain for comparison against the Space Shuttle specification for EMI.

Two perpendicular antennae were used to find the direction and strength of the electromagnetic field. Thus antennae A and B were mounted in orthogonal directions to measure the components (signal strength vs time) of arc-induced electromagnetic radiation generated in each of the respective directions.

Figures 4a and 4b show typical electromagnetic signatures picked up by the horizontally mounted insulated antenna, as well as the resultant electromagnetic frequency spectrum obtained by the

horizontal antenna. Similar data were recorded for the vertical antenna (Figs. 5a and 5b). Note that the magnitude of the frequency plots is in relative units. The E-field strength was estimated as 0.5 V/m/MHz. The EMI standards for the ISS are given in units of dB [μV/m/MHz].[9,10] The EMI levels for the horizontal and vertical antennae exceed the EMI standards set forth for the ISS and the Space Shuttle.[9] Figures 6a and 6b show the EMI level of arcs on an anodized aluminum plate converted to units of decibels. Figure 6a demonstrates quantitatively that the safe EMI level specified for the Space Shuttle is exceeded. Figure 6b shows similar data for payloads in the Shuttle payload bay, which are held to a more rigorous EMI standard. Note that data plotted in Figs. 6a and 6b are the result of 34 separate ground-based antennae measurements of EMI levels due to arcs on anodized aluminum plates.

The next set of measurements involved determining the travel time of the expanding plasma cloud caused by the arcing process. Noninsulated probes were used to pass the conducted emissions. As already discussed, when an arc strikes, a quasineutral cloud of material is ejected into the ambient plasma. Experiments have shown that a single arc on an anodized aluminum plate may generate as many as 10^{15} atoms of aluminum into the surrounding plasma.[11]

It is possible to measure the overall time response of the probe to the arcing process and hence make travel time estimates based on the difference in time Δt between when an arc event initially occurs and when the wire probe finishes sensing the perturbations causing the arc (Fig. 7). The upper trace displays the initial arc event, which is initially triggered by an arc on plate #1. The lower trace, which was simultaneously triggered, displays what is sensed by the wire probe. It is important to note that the initial arc trigger occurs at point A. The plasma cloud oscillations are fully developed by the time point P is reached. Point B designates the time just before the rise of the small pulse at point E is sensed. The small oscillation at point E is a result of electrical field fluctuations generated by breakdown of the anodized coating. This pulse at point E marks the end of the arcing process. Hence, the travel time is equal to the difference in time Δt between points A and B. Table 2 tabulates the plasma cloud travel times for various probes. Because the distances from the plate to each probe are known (see Table 1), the average velocity of the expanding plasma cloud can be calculated. These values are shown in Table 2. A statistical analysis of the plasma-cloud expansion velocities shown in Table 2 yields a mean propagation velocity, $v = (19.4 \pm 3.5)$ km/s. Note that one could have judiciously chosen the peak values at points P and E for the travel time estimates. In this case the travel time estimate would have been shorter than reported in Table 2.

The final set of experiments involved induced arcing between two parallel plates of anodized aluminum in close proximity. The purpose of these experiments was to verify that an initiating arc

Table 2 Tabulated results for plasma cloud travel times, velocity, and frequency

Probe type	$\Delta t = (\tau - \tau_0)$, μs	$v = (\Delta x/\Delta t)$, km/s	$f = 1/\Delta t$, kHz
Wire probe 1	28.8	19.8	34.7
Wire probe 1	34.1	16.8	29.3
Wire probe 1	28.7	19.9	34.7
Wire probe 1	30.9	18.5	32.4
Wire probe 2	37.3	20.8	26.8
Wire probe 2	34.2	22.7	28.2
Wire probe 2	32.5	23.8	30.8
Wire probe 2	35.0	22.1	28.6
Sphere LP2	31.3	15.6	31.9
Sphere LP2	34.1	15.6	29.3
Sphere LP2	34.3	14.3	29.2
Sphere LP2	20.3	24.1	49.3

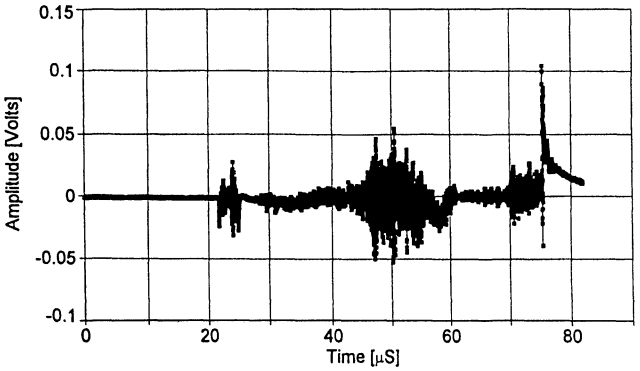

Fig. 4a Electromagnetic signature resulting from arc. Signal trace shown was acquired from the horizontal antenna (antenna A).

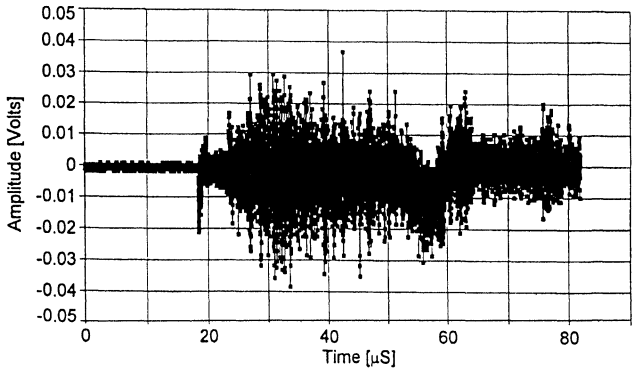

Fig. 5a Electromagnetic signature resulting from arc. Signal trace shown was acquired from the vertical antenna (antenna B).

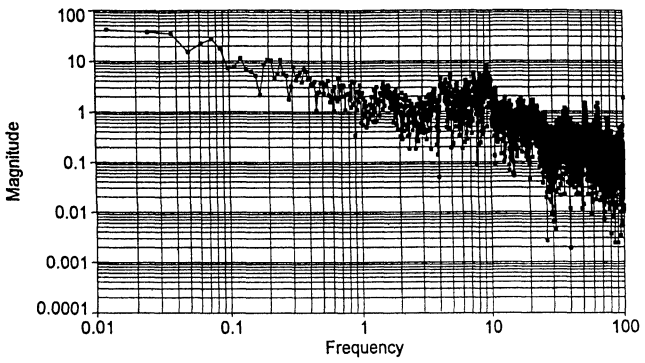

Fig. 4b Resultant electromagnetic frequency spectrum for the horizontal antenna. Displayed waveform was obtained from the Fourier transform of signal trace in Fig. 4a. (Note: frequency is in megahertz, and vertical scale is given in relative units.)

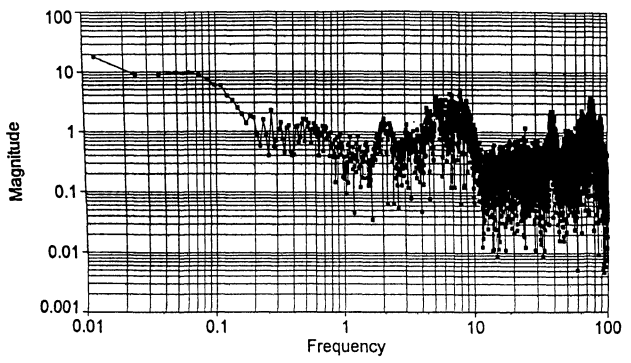

Fig. 5b Resultant electromagnetic frequency spectrum for the vertical antenna. Displayed waveform was obtained from the Fourier transform of signal trace in Fig. 5a. (Note: frequency is in megahertz, and vertical scale is given in relative units.)

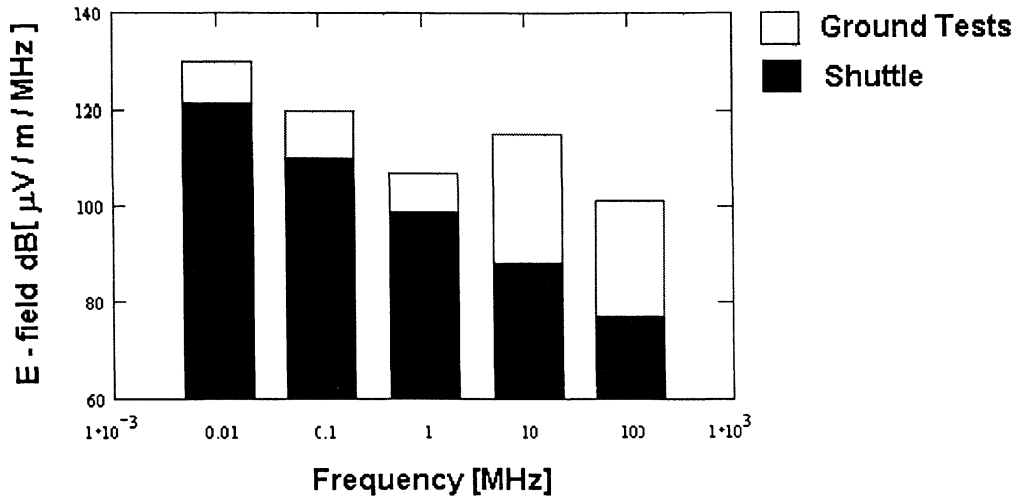

Fig. 6a Comparison of maximum EMI levels set for the Shuttle and EMI levels obtained from arcs at approximately 1 m distance in ground testing at LeRC (see Ref. 11 for details).

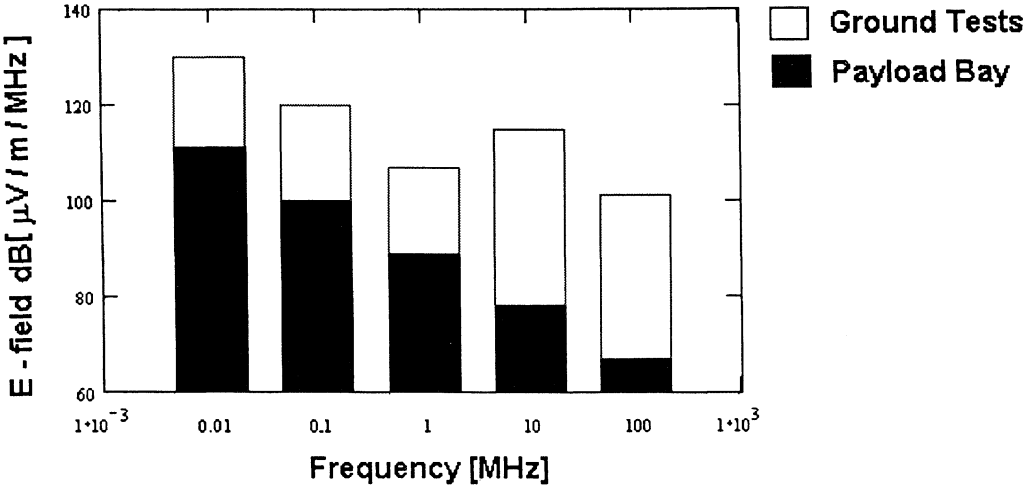

Fig. 6b Comparison of maximum EMI levels set for payload in the Shuttle payload bay and EMI levels obtained from arcs at ≈1 m distance from the plate at LeRC (see Ref. 11 for details).

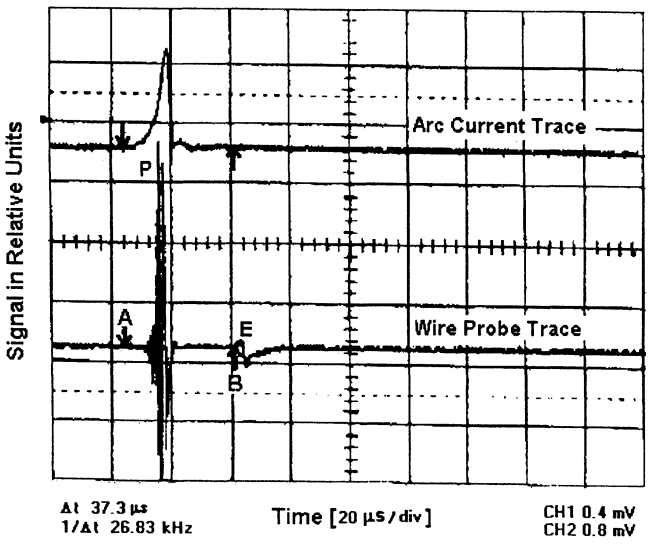

Fig. 7 Typical signal traces obtained from plasma cloud propagation tests (plate # 1: $\phi_b = -400$ V, $C = 47$ μF, $R = 100$ kΩ).

on plate A would cause an arc to be triggered on plate B. Plate A was negatively biased at a potential above the arcing threshold. Plate B was set to a less negative potential, just under the arcing threshold. It was felt an arc triggered on plate A could temporally pull plate B more negative than the bias potential set on plate B. The net voltage drop could cause electrical breakdown of the anodized coating on plate B.

For these tests the sulfuric-acid anodized coatings (Type II; MIL-A-8265E) were abandoned for some of the chromic-acid anodized coatings (Type I; MIL-A-8265E) used in the previous summer's experiments. The chromic-acid anodized plates arced at nearly half the voltage (−200 V) of the sulfuric-acid anodized plates. (The sulfuric-acid anodized samples were found to arc at approximately −400 V.) Because the chromic-acid anodized plates were manufactured to the same coating thickness, $\Delta x = 2.5$ μm, this equates to a 50% reduction in the E-field strength, or $E = 7.9 \times 10^7$ V/m, before arcing can occur in the chromic-acid anodized coatings. As a result, the chromic-acid anodized coatings better represent the actual charging potentials that may be seen on ISS when no plasma contactor is present. Because only a small amount of the anodized material was available at the time of these tests, the samples were cut into smaller 18 × 18 cm plates for these experiments. Sample pairs were mounted in the tank with a separation of 25 and 50 cm between

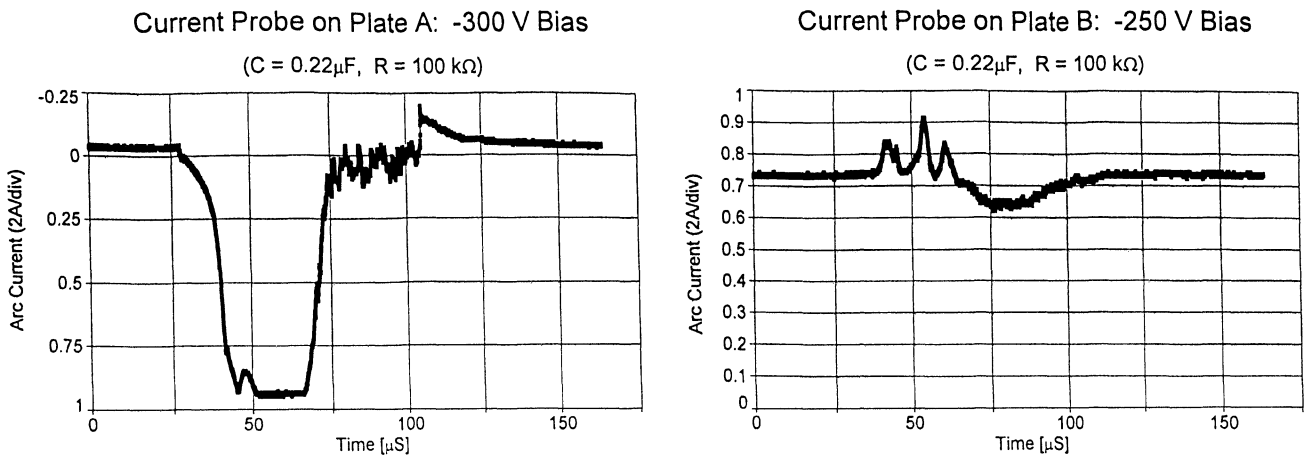

a) Plate A b) Plate B

Fig. 8 Arc pulses recorded on two independently biased parallel plates. (Note: distance between plates is 50 cm, and no measured delay was observed.)

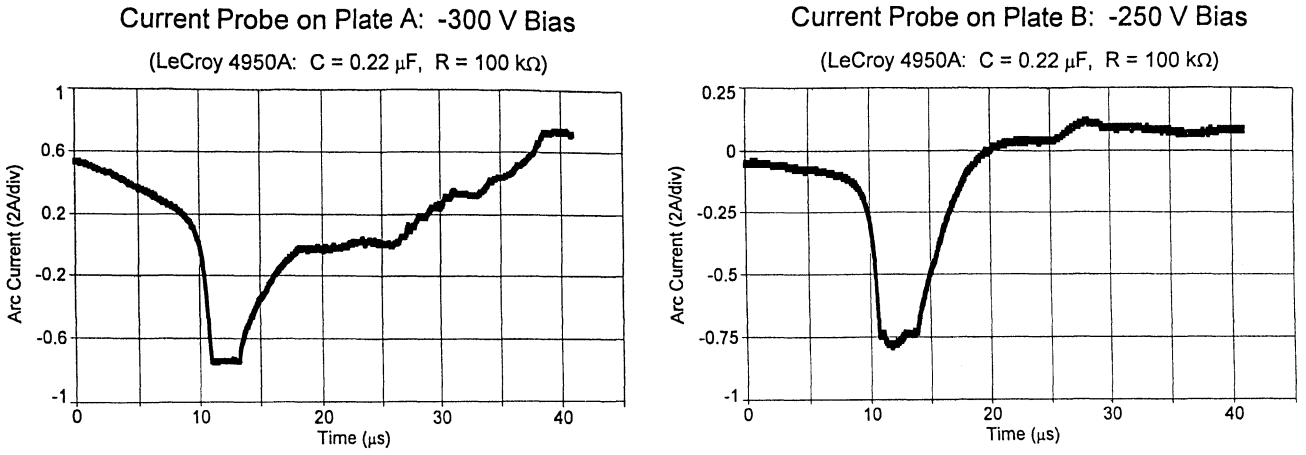

a) Plate A b) Plate B

Fig. 9 Induced arcing between two independently biased parallel plates. (Note: distance between plates is 25 cm, and no measured delay was observed.)

each parallel plate pair. One parallel plate in each pair was biased at −250 V potential. The remaining plate in each pair was biased at −300 V.

Figures 8a and 8b show the current registered by two independently biased parallel plates separated by 50 cm. Figures 9a and 9b demonstrate induced arcing between two independently biased parallel plates at a distance of 25 cm from one another. Note that the arc pulses are of comparable height here. The delay time could not be measured because of the timescale of the waveforms. What is certain is that the time delay is not because of influences caused by expansion of the plasma cloud, which is on the order of 20–40 μs. Hence, arcs on plate A and plate B appear to be simultaneously triggered. In Figs. 8 and 9 the initiating arc is believed to occur on plate A because plate B is below the arcing threshold.

Conclusion

Much valuable information important to the ISS, spacecraft designers, and the scientific community in general has been obtained as a result of these tests. With the current setup we have been able to record successfully the electromagnetic radiation spectrum resulting from the arcing process. The frequency spectrum peaks between 8 and 10 MHz, and the magnitude of interference exceeds the EMI technical specifications set for Space Shuttle operation. Accurate estimates of the time of travel of the expanding plasma cloud resulting from the arcing process also were made. Measurements have ascertained that the velocity of the expanding plasma cloud (19.4 ± 3.5 km/s) is somewhat lower than earlier estimates of 25–30 km/s (Ref. 1). These velocities are highly dependent on the points chosen for the travel time estimates. Finally, induced arcing between two independently biased anodized plates is possible. Induced arcing could have serious consequences for high-power instrument payloads operating in the Shuttle payload bay.

References

[1]Vaughn, J. A., Carruth, M. R., Jr., Katz, I., Mandell, M. J., and Jongeward, G. A., "Electrical Breakdown Currents on Large Spacecraft in Low Earth Orbit," *Journal of Spacecraft and Rockets*, Vol. 31, No. 1, 1994, pp. 54–59.

[2]Kennerude, K. L., "High Voltage Array Experiments," NASA CR-121280, March 1994.

[3]McCoy, J. E., and Konradi, A., "Sheath Effects Observed on a 100 Meter High Voltage Panel in Simulated Low Earth Orbit," *Proceedings of Spacecraft Charging Technology 1978*, NASA CP-2071, 1978, pp. 201–210.

[4]Robinson, P., and Whittlesey, A., "Electrostatic Charging Characteristics of Thermal Control Paints as a Function of Temperature," *Proceedings of Space Charging Technology 1980*, NASA CP 2182, 1980, pp. 309–319.

[5]Leung, P., "The Electrical Conductivity of ZOT After a Long Term Exposure to Thermal Vacuum Environment," *Proceedings of Spacecraft Charging Technology Conference 1989*, NASA, 1989, pp. 166–173.

[6]"Anodic Coatings for Aluminum and Aluminum Alloys," Systems Engineering and Standardization Dept., U.S. Naval Air Engineering Center,

Military Specification MIL-A-8625E, Navy-AS MFFP-0368, Lakehurst, NJ, April 1988, pp. 1–18.

[7]Carruth, M. R. Jr., Vaughn, J. A., and Gray, P. A., "Experimental Studies of Spacecraft Arcing," AIAA Paper 92-0820, Jan. 1992.

[8]Carruth, M. R., Jr., Vaghn, J. A., Holt, J. M., Werp, R., and Sudduth, R. D., "Plasma Effects on Passive Thermal Control Coatings of Space Station Freedom," AIAA Paper 92-1685, March 1992.

[9]Vayner, B. V., Doreswamy, C. V., Ferguson, D. C., Galofaro, J., and Snyder, D. B., "Arcing on Aluminum Anodized Plates Immersed in Low-Density Plasmas," *Journal of Spacecraft and Rockets*, Vol. 35, No. 6, 1998, pp. 805–811.

[10]Vayner, B.V., Ferguson, D. C., and Snyder, D. B., "Electromagnetic Radiation Generated by Arcing in Low Density Plasma," NASA TM-107217, July 1996.

[11]Vayner, B.V., Ferguson, D. C., and Galofaro, J., "The Spacecraft Surfaces Degradation and Contamination Caused by Arcing in Low Density Plasmas," *Proceedings of XVIVth International Symposium on Discharges and Electrical Insulation in Vacuum*, Vol. 2, Eindoven Univ. of Technology, Eindhoven, The Netherlands, 1998, pp. 824–827.

I. D. Boyd
Associate Editor